A general purpose reporter for cations: absorption, fluorescence and electrochemical sensing of zinc(II)

Andrew C. Benniston,* Anthony Harriman, Donald J. Lawrie, Annabelle Mayeux, Karen Rafferty and Owen D. Russell

Molecular Photonics Laboratory, School of Natural Sciences – Chemistry, Bedson Building, University of Newcastle, Newcastle upon Tyne, UK NE1 7RU. E-mail: a.c.benniston@ncl.ac.uk; Fax: +44 (0)191 222 8664; Tel: +44 (0)191 222 5706

A fluorescent sensor has been synthesized that comprises a pyrene moiety tethered to a [2,2′:6′,2″]-terpyridyl ligand *via* a diethynylated thiophene linker. This multicomponent supermolecule is highly emissive in solution but addition of Zn^{2+} cations results in a drastic decrease in the fluorescence yield. Complexation between Zn^{2+} cations and the vacant terpyridyl ligand has been confirmed by NMR spectroscopy and by electrospray mass spectrometry. The ES-MS results provide strong support for the formation of both 1 : 1 and 1 : 2 (metal : ligand) complexes in solution. Complexation is further evidenced by a pronounced shift in the absorption spectrum, by the appearance of a long-wavelength band in the fluorescence spectrum and by cyclic voltammetry. On the basis of UV-visible spectrophotometric titrations, overall binding constants of $\log \beta_1 \approx 5.1$ and $\log \beta_2 \approx 9.9$ were derived for the 1 : 1 and 1 : 2 complexes, respectively, in acetonitrile solution. The possible application of this system as a generic chemical sensor for cationic species is mentioned.

Introduction

Selective molecular recognition and highly responsive signalling of physical and/or chemical interactions are two prime requisites for any efficient analytical sensor.[1] To meet the first objective, analyte binding can be realized using hosts such as cyclodextrins,[2] crown ethers,[3] aza-macrocycles,[4] chelates,[5] calixarenes,[6] cyclophanes[7] and related superstructures bearing central cavities. In order to report on molecular interactions such hosts are further functionalized with secondary groups that are perturbed upon guest binding. This perturbation is recorded by a change in reduction potential[8] or a modification of the optical properties, such as the absorption maximum,[9] fluorescence yield,[10] circular dichroism spectrum[11] or degree of circularly polarised luminescence,[12] of the reporter. Optical signalling *via* luminescence quenching or enhancement is a particularly attractive method that has been utilised in a number of systems developed to date.[13] The ultimate sensitivity of a luminescence-based reporter is set by the difference in signal between the 'on' and 'off' states. To maximise sensitivity, it is essential that one of these two states is 'dark' while the other is 'bright'. This realisation has led to the extensive use of aromatic polycycles such as pyrene as the fluorescent reporter. In fact, pyrene is highly fluorescent, both as a monomer and an excimer, and readily undergoes electron-transfer quenching.[14] Hence, pyrene has found wide usage as a fluorescent sensor for sugars,[15] alkali metals,[16] iodide ions,[17] dioxygen,[18] bile acids,[19] and mercuric ions.[20]

We have become interested in the design of a general fluorescent sensor for detecting trace metal cations in solution. In common with many other systems, we have selected pyrene as the basic fluorophore and poly(pyridine) ligands as the recognition site. It is known that these two units operate independently to bind and detect adventitious cations in solution. When connected together *via* a conjugated linker, the two terminals act cooperatively in that the normal pyrene-like fluorescence is replaced with charge-transfer emission.[21] This effect greatly enhances the analytical potential of the system since the recognition site is now part of the fluorophore. However, the 'on' state was not sufficiently bright for the device to be viable as an analytical tool. We now report that replacing the ethynylene linker with 2,5-diethynylated thiophene has a major influence on the photophysical properties of the free ligand. Thus, the pyrene functionalised ligand L_1 has considerable scope as a general purpose sensor for cations. We illustrate the overall properties of this system by reference to detection of $Zn(ClO_4)_2$ in CH_3CN, but this is representative of much more versatile binding behaviour.

Numerous other fluorescence-based molecular systems are available for the detection of zinc(II) ions in solution. Many such sensors are selective towards zinc(II) cations by varying the pH[22–24] and can operate at the nanomolar range. Other systems suffer from poor 'on–off' differentials,[25] but Fages and co-workers[26] have described two highly conjugated pyrene-2,2′-bipyridine rod-like molecules whose strong fluorescence is heavily quenched on addition of zinc(II) cations. There are clear similarities between these latter systems and L_1. We focus here on the novel features of L_1 with respect to binding of zinc(II) cations and will report later on the general-purpose sensing properties of this class of compound. An added advantage of L_1 is that cation binding can be visualised by changes in the UV-visible absorption spectrum and by the appearance of a new wave in the cyclic voltammograms observed during electroreduction.

Experimental

All chemicals were purchased from Aldrich Chemicals Co. and were used as received. Solvents were dried by standard literature methods[27] before being distilled and stored under nitrogen over 4Å molecular sieves. ^{1}H and ^{13}C NMR spectra were recorded with a JEOL Lambda 500 spectrometer. Routine mass spectra and elemental analyses were obtained using in-house facilities. 4-Ethyl-5-iodothiophen-2-ylethynyltrimethylsilane (1),[28] 1-ethynylpyrene (2)[29] and trifluoromethane sulfonic acid [2,2′:6′,2″]terpyridin-4′-yl ester (5)[30] were prepared and purified by literature methods.

Cyclic voltammetry experiments were performed using a fully automated HCH Instruments Electrochemical Analyzer, and a three electrode set-up consisting of a glassy carbon working electrode, a platinum wire counter electrode and an SCE reference electrode. All experiments were performed in dry CH_3CN containing tetra-*N*-butylammonium tetrafluoroborate (0.2 mol dm^{-3}) as background electrolyte. Absorption spectra

were recorded with an Hitachi U3310 spectrophotometer while corrected fluorescence spectra were recorded with an Hitachi F4500 spectrophotometer. All fluorescence measurements were made using optically dilute solutions and were corrected for spectral imperfections of the instrument by reference to a standard lamp. Quantum yields were determined relative to either 9,10-diphenylanthracene in benzene[31] or ruthenium(II) *tris*(2,2′-bipyridine) in acetonitrile.[32] Time-resolved fluorescence measurements were made with a Spex Fluorolog tau-3 spectrophotometer.

Spectrophotometric titrations were performed by adding small quantities of a standard solution of zinc perchlorate in acetonitrile to a dilute solution of L_1 in acetonitrile. The course of reaction was followed either by integrating the entire emission band or by measuring the fluorescence intensity at fixed wavelength. It should be stressed that very low concentrations of cation are needed to extinguish fluorescence. The presence of oxygen had no effect on the titration but it was essential to avoid contamination by acid or other cations. Similar titrations were made by following changes in the absorption spectrum upon addition of small amounts of zinc perchlorate. The latter results were analysed using SPECFIT. A spreadsheet was constructed using absorbance values collected at 160 different wavelengths within the range 330–490 nm and for 30 different concentrations of cation. The effect of minor dilution of the sample was corrected and the results were subject to vector analysis in order to determine the probable number of components. Known spectra of the free ligand and 1 : 1 complex were used to assist data analysis. Kinetic studies with made by the stopped-flow method using an Applied Photophysics Ltd. Instrument.

Analysis of the fluorescence spectral titration data was made as follows: first, a complete spectral analysis was made using SPECFIT with the known spectra for the free ligand and for the final 1 : 2 complex. This analysis allowed determination of the relative fluorescence yields of the free ligand and of the 1 : 2 complex and of the fluorescence spectrum for the latter species. The analysis indicated that only two fluorescing species were involved. Secondly, a quantitative analysis was made by fitting the fluorescence intensity at a single wavelength, measured at different cation concentrations, to a set of model equations. Stability constants were derived by fitting experimental data collected at 10 different wavelengths and for at least 20 different cation concentrations. The results from three separate titrations were averaged to give the quoted binding constants.

Computational studies were made with the Gaussian-03 package, with visualisation *via* GaussView. Calculations were run on a fast PC. Geometry optimisation was made using the ONOIM (MM:MO) module for the solute in a bath of water molecules. Excitation energies were calculated using the CASSCF method. The practical active space was restricted to five occupied and six unoccupied molecular orbitals. Again, water was used as the solvent.

(4-Ethyl-5-pyren-1-ylethynylthiophen-2-ylethynyl)trimethylsilane (3)

1-Ethynylpyrene (1.30 g, 5.77 mmol), 4-ethyl-5-iodothiophen-2-ylethynyltrimethylsilane (2.13 g, 6.35 mmol), bis(triphenylphosphine)palladium(II) dichloride (203 mg, 290 μmol) and copper(I) iodide (28 mg, 150 μmol) were mixed and thoroughly deoxygenated under vacuum. After degassing, the reactants were dissolved in deoxygenated THF (100 mL) and the resultant solution stirred for 10 min before addition of diisopropylamine (50 mL). The solution was stirred at room temperature for a further 2 h before being quenched by addition of water (100 mL). The organic layer was separated and the aqueous layer was washed with diethyl ether (3 × 100 mL). The combined organic layers were washed with water until the washings were neutral. The organic layer was then dried over MgSO$_4$ and

evaporated to give the crude product. Purification was achieved by column chromatography (silica gel, light petroleum–dichloromethane (0 to 20%)) to yield 1.31 g (52%) of the desired product as a yellow oil. ^{1}H NMR (500 MHz, CDCl$_3$): δ 0.26 (s, 9H, SiMe$_3$), 1.26 (t, 3H, J = 7.6 Hz, CH$_3$), 2.72 (q, 2H, J = 7.6 Hz, CH$_2$), 7.18 (s, 1H, CH$_{thio}$), 8.11 (m, 8H, CH$_{pyrene}$) 8.55 (d, 1H, J = 8.8 Hz, CH$_{pyrene}$). ^{13}C NMR (125.65 MHz, CDCl$_3$): δ 0.00 (3C), 14.39, 22.95, 29.33, 53.86, 88.43, 93.07, 96.86, 102.47, 117.23, 119.91, 123.35, 124.37, 124.62, 125.46, 125.77, 125.83, 126.37, 127.30, 128.42, 128.57, 129.52, 131.13, 131.54, 131.91, 132.37, 150.05. HR-MS: calc. for C$_{29}$H$_{24}$SSi: 432.1396, found: 432.1368.

3-Ethyl-5-ethynyl-2-pyren-1-ylethynylthiophene (4)

A solution of **3** (1.21 g, 2.79 mmol) and potassium hydroxide (630 mg, 11.20 mmol) (dissolved in the minimum amount of water (2 mL)) in methanol (15 mL) and diethyl ether (30 mL) was stirred at room temperature for 24 h before addition of water (150 mL). The aqueous layer was extracted with diethyl ether and the organic extracts were combined, dried over MgSO$_4$ and evaporated to give 1.00 g (99%) of the desired product as a yellow solid, which was used without further purification. ^{1}H NMR (500 MHz, CDCl$_3$): δ 1.29 (t, 3H, J = 7.6 Hz, CH$_3$), 2.76 (q, 2H, J = 7.5 Hz, CH$_2$), 3.52 (s, 1H, CH), 7.22 (s, 1H, CH$_{thio}$), 8.13 (m, 8H, CH$_{pyrene}$) 8.58 (d, 1H, J = 9.1 Hz, CH$_{pyrene}$). ^{13}C NMR (125.65 MHz, CDCl$_3$): δ 14.51, 22.83, 29.33, 53.92, 76.18, 84.33, 87.99, 93.03, 117.01, 118.35, 123.75, 124.29, 124.47, 124.55, 125.35, 125.78, 126.32, 127.23, 128.40, 128.55, 129.48, 131.06, 131.25, 131.53, 131.87, 150.41. HR-MS: calc. for C$_{26}$H$_{16}$S: 360.0972, found: 360.0962.

3-Hexadecyl-2-iodothiophene (6)

Under a dry N$_2$ atmosphere, cetylbromide (16.8 ml) in anhydrous Et$_2$O (200 ml) was added dropwise to magnesium turnings (1.096 g, 47.6 mmol) at room temperature. The resultant mixture was stirred for 1 h, and transferred *via* a cannula to a solution of 3-bromothiophene (2.85 ml) and 1,3-bis(diphenylphosphino)propane nickel(II) chloride (18 mg, 0.034 mmol) in dry Et$_2$O at −78 °C. The mixture was allowed to warm to room temperature and left to stir overnight. The solution was poured into water (50 ml) containing a few drops of 2 M HCl, and extracted with Et$_2$O (5 × 25 ml). The combined organic extracts were washed with brine, separated, and dried over MgSO$_4$. Removal of the solvent afforded a crude solid which was purified by flash chromatography (silica gel) with light petroleum as eluent. Yield 4.22 g, 45%. ^{1}H NMR (CDCl$_3$): δ 0.89 (t, 3H, J = 6.5 Hz, CH$_3$), 1.27 (br, s, 26H, CH$_2$), 1.61 (m, 2H, CH$_2$), 2.64 (t, 2H, J = 7.5 Hz, CH$_2$), 6.93 (m, 2H. CH$_{thio}$), 7.24 (m, 1H, CH$_{thio}$). ^{13}C NMR (CDCl$_3$): δ 14.42 (1C), 23.00 (1C), 29,66 (3C), 29.77 (8C), 30.58 (1C), 30.87 (1C), 32.23 (1C), 120.04 (1C), 125.29 (1C), 128.58 (1C). HR-MS: calc. for C$_{20}$H$_{36}$S: 308.2538, found 308.2525.

To a solution of the above compound (4.22 g, 13.7 mmol) in benzene (7.6 mL) at 0 °C was added mercuric oxide (2.967 g, 13.7 mmol). After standing for a few minutes, a solution of iodine (3.824 g, 15.07 mmol) in dried CH$_2$Cl$_2$ (3.8 mL) was added dropwise. The mixture was stirred overnight at room temperature, followed by filtration through Celite to remove unreacted starting material. The filtrate was poured into water (10 mL) and the aqueous layer extracted with Et$_2$O (5 × 10 mL). The combined organic extracts were washed with brine, separated, and dried over MgSO$_4$. Removal of the solvent afforded a crude solid which was purified by flash chromatography (silica gel) with light petroleum as eluent. Yield 3.05 g, 51%. ^{1}H NMR (CDCl$_3$): δ 0.81 (t, 3H, J = 6.2 Hz, CH$_3$), 1.18 (br, s, 26H, CH$_2$), 1.51 (m, 2H, CH$_2$), 2.47 (t, 2H, J = 7.5 Hz, CH$_2$), 6.68 (d, 1H, J = 5.4 Hz, CH$_{thio}$), 7.30 (d, 1H, J = 5.4 Hz, CH$_{thio}$). ^{13}C NMR (CDCl$_3$): δ 14.45 (1C), 23.01 (1C), 29.66 (3C), 29.99 (8C), 30.59 (1C), 30.87 (1C), 32.23 (1C), 120.04 (1C), 125.09 (1C), 125.09

(1C), 128.59 (1C). HR-MS: calc. for $C_{20}H_{35}IS$: 434.1504, found 434.1491.

4-Hexadecyl-2-pyren-1-ylethynylthiophene (L_2)

A mixture of 1-ethynylpyrene (250 mg, 1.1 mmol), **6** (529.5 mg, 1.22 mmol), bis(triphenylphosphine)palladium(II) dichloride (38.96 mg, 0.055 mmol) and copper(I) iodide (5.29 mg, 0.028 mmol) was deaerated under vacuum. Anhydrous THF (25 mL) and dried diisopropylamine (5 mL) were added and the reaction mixture stirred at room temperature for 2 days. Water (10 mL) was added to the solution, which was subsequently extracted with dichloromethane (5 × 10 mL). The combined organic extracts were dried over $MgSO_4$ and evaporated to afford a crude material which was purified by flash chromatography (silica gel) with petrol:dichloromethane (9 : 1) as eluent. Yield 120 mg, 36%. A spectroscopically pure sample was obtained by recrystallisation from light petroleum followed by preparative TLC (silica gel, light petroleum). ^{1}H NMR (CDCl$_3$): δ 1.06 (t, 3H, $J = 6.5$ Hz, CH$_3$), 1.29 (m, 26H, CH$_2$), 1.73 (m, 2H, CH$_2$), 2.87 (t, 2H, $J = 7.5$ Hz, CH$_2$), 6.99 (d, 1H, $J = 5.2$ Hz, CH$_{thio}$), 7.19 (d, 1H, $J = 5.0$ Hz, CH$_{thio}$), 8.0–8.3 (m, 8H, CH$_{pyrene}$), 8.55 (d, 1H, $J = 9.1$ Hz, CH$_{pyrene}$). ^{13}C NMR (CDCl$_3$): δ 14.52 (1C), 23.09 (1C), 29.75 (1C), 29.87 (1C), 30.08 (9C), 30.29 (1C), 30.90 (1C), 32.32 (1C), 88.57 (1C), 94.94 (1C), 118.32 (1C), 118.98 (1C), 124.95 (1C), 124.95 (1C), 125.33 (2C), 125.94 (2C), 126.65 (2C), 127.66 (1C), 128.51 (1C), 128.73 (1C), 128.86 (1C), 129.71 (1C), 131.53 (1C), 131.69 (1C), 131.92 (1C0, 148.44 (2C). HR-MS: calc. for $C_{38}H_{44}S$: 532.3164, found 532.3157.

4′-(4-Ethyl-5-pyren-1-ylethynylthiophen-2-ylethynyl)-[2,2′:6′,2″]terpyridine (L_1)

A mixture of **4** (100 mg, 277 µmol), **5** (117 mg, 305 µmol) and tetrakis(triphenylphosphine)palladium(0) (16 mg, 1.3 µmol) was degassed thoroughly under vacuum. After degassing, the reactants were dissolved in deoxygenated THF (10 mL) and the resultant solution was stirred for 20 min before addition of diisopropylamine (7 mL). The solution was refluxed at 95 °C for 2 days and then quenched by addition of water (50 mL). The organic layer was separated and the aqueous layer was washed with dichloromethane (5 × 50 mL). The organic residues were combined and washed with water until the washings were neutral. The organic layer was dried over $MgSO_4$ and evaporated to give the crude product. Purification was made by column chromatography (basic alumina, light petroleum–dichloromethane (0 to 50%)) to yield 106 mg (51%) of the desired product as an orange solid. ^{1}H NMR (500 MHz, CDCl$_3$): δ 1.37 (t, 3H, $J = 7.6$ Hz, CH$_3$), 2.88 (q, 2H, $J = 7.6$ Hz, CH$_2$), 7.29 (s, 1H, CH$_{thio}$), 7.39 (qd, 2H, $J = 5.6$ Hz, $J' = 1.5$ Hz, CH$_{terpy}$), 7.90 (td, 2H, $J = 7.7$ Hz, $J' = 1.7$ Hz, CH$_{terpy}$), 8.15 (m, 8H, CH$_{pyrene}$) 8.57 (s, 2H, CH$_{terpy}$), 8.60 (d, 1H, $J = 9.2$ Hz, CH$_{pyrene}$) 8.65 (d, 2H, $J = 7.9$ Hz, CH$_{terpy}$), 8.76 (d, 2H, $J = 3.9$ Hz, CH$_{terpy}$). ^{13}C NMR (125.65 MHz, CDCl$_3$): δ 14.72, 23.10, 86.41, 86.15, 93.84, 94.67, 117.00, 118.75, 121.29 (2C), 122.27 (2C), 124.07 (2C), 124.28, 124.46, 124.57, 124.94, 125.34, 125.73, 125.81, 126.31, 127.23, 128.41, 128.59, 129.52, 131.07, 131.24, 131.55, 131.88, 132.57, 133.10, 136.97 (2C), 149.18 (2C), 150.61, 155.54 (2C), 155.64 (2C). HR-MS: calc. for $C_{41}H_{25}N_3S$: 591.1769, found 591.1783. CHN analysis: calc. (found) for $C_{41}H_{25}N_3S·H_2O$: C, 80.76 (80.10); H, 4.46 (4.26); N, 6.89 (6.97)%.

Results and discussion

General considerations

The ligand L_1 has been designed as a general purpose fluorescent reporter for cations in solution. The appended terpyridine ligand is intended to serve as a receptor for adventitious cations, including protons. Pyrene is used as the fluorescent label but the key component in the overall supermolecule is the central diethynylated thiophene residue. It is known that this latter unit is a good electronic conductor[33] and its inclusion as a component in L_1 is to promote electronic coupling between the terminal sites. In this way, cation complexation should be registered by a marked change in fluorescence yield. Also, thiophene is readily functionalised so as to provide for water solubility or anchoring to a surface and it can be electropolymerised.[34] These latter features become important when considering how best to incorporate the sensor in a practical device.

Outlined in Scheme 1 is the synthetic procedure used for preparation of the fluorescent reporter ligand L_1 and the control compound L_2. Linking the thiophene-based derivative **1** to the pyrene-containing segment **2** proceeded smoothly under standard cross-coupling conditions to afford intermediate **3** in a respectable 52% yield. Removal of the TMS protecting group afforded **4** in essentially quantitative yield, prior to its tethering to the terpyridine-based precursor **5** using standard Sonogashira coupling conditions.[35] This latter step was realised in 51% overall yield. The target compound is reasonably soluble in common organic solvents and in acidic aqueous solution. Compound L_2 was prepared by coupling **2** with the thiophene derivative **6**. It should be noted that the substitution pattern around the thiophene residue differs in L_1 and L_2.
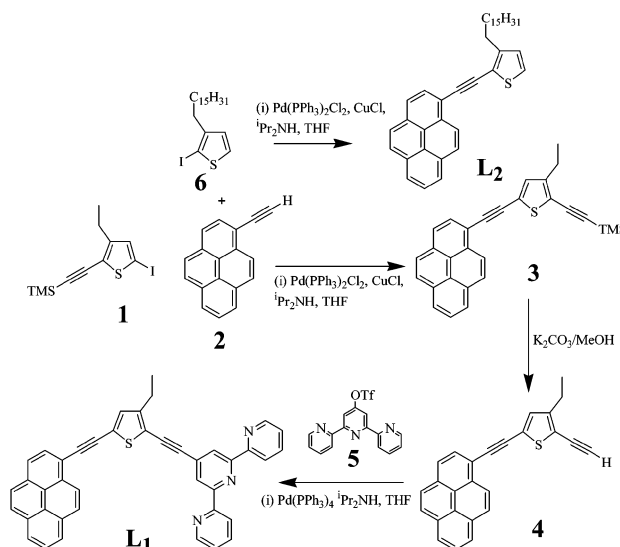

Scheme 1 Synthetic procedure used in the synthesis of the fluorescent reporter L_1 and control compound L_2.

^{1}H NMR spectroscopy

The binding affinity of L_1 towards Zn^{2+} cations was monitored by ^{1}H NMR spectroscopy in a CDCl$_3$–(CD$_3$)$_2$SO mixture at ambient temperature. Illustrated in Fig. 1 is the aromatic region of L_1 before and after the addition of sufficient $Zn(ClO_4)_2$ to form the expected 1 : 2 (metal : ligand) complex. Specific proton resonances corresponding to pyrene, thiophene and terpyridyl groups are affected and undergo significant chemical shifts. The singlet due to the proton on the thiophene nucleus undergoes an upfield shift of *ca.* 0.04 ppm, which would suggest that there is a decrease in the electron current density at this site.[36] Comparable upfield shifts were observed for several of the pyrene resonances. That the singlet corresponding to the terpyridyl protons proximal to the acetylene group undergoes a major downfield shift (*ca.* 0.09 ppm) is consistent with enhanced deshielding caused by an increased ring-current effect at the central pyridine ring.

These various perturbations of the ^{1}H NMR spectrum serve to indicate two important effects: First, it is evident that L_1 binds added Zn^{2+} cations with high affinity. Presumably, co-ordination takes place at the vacant terpyridyl site but, while the NMR results are consistent with this hypothesis, this point
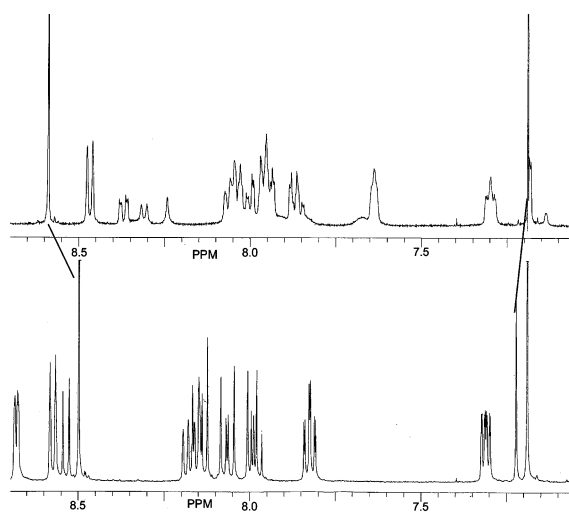
Fig. 1 Partial ^{1}H NMR (500 MHz) spectra of the aromatic region of $\mathbf{L_1}$ in the presence (top) and absence (bottom) of $Zn(ClO_4)_2$.

has not been established by experiment. Second, it is clear that there is strong electronic coupling along the molecular axis, especially following coordination of the cation. This effect is apparent from the effect that cation binding has on those NMR signals due to (supposedly) remote sites, such as the pyrene chromophore. In turn, this suggests to us that the ground state of $\mathbf{L_1}$ is relatively polar because of intramolecular charge transfer from pyrene to either the central thiophene residue or the terminal terpyridyl site.

Electrochemical sensing

Cyclic voltammograms recorded for $\mathbf{L_1}$ in deoxygenated acetonitrile containing tetra-*n*-butylammonium tetrafluoroborate (0.2 mol dm^{-3}), as background electrolyte, showed several regions of interest (Scheme 2). Firstly, on oxidative scans an irreversible peak can be discerned at 1.31 V *vs.* Ag/AgCl. Based on literature data,[29] this oxidation step is most likely due to one-electron oxidation of the pyrene subunit. The process is irreversible because of rapid formation of the corresponding pyrene dimer π-radical cation by association with a
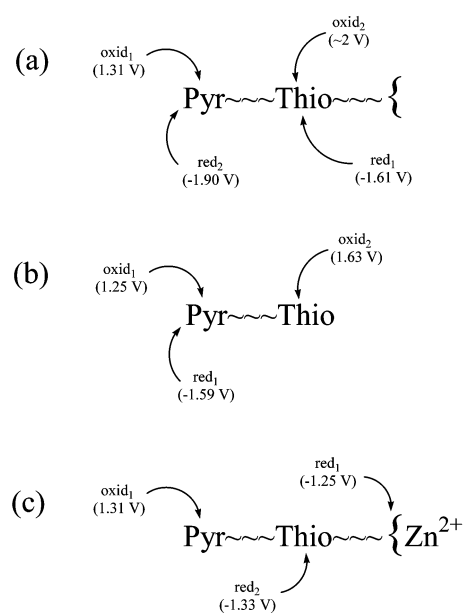
Scheme 2 Pictorial representation of the electrochemical processes relevant to (a) $\mathbf{L_1}$, (b) $\mathbf{L_2}$ and (c) the Zn^{2+} complex formed with $\mathbf{L_1}$. Note, in panel (c) the reduction potentials were obtained by fitting the broad peak to successive one-electron waves.

second pyrene moiety.[37] It should be noted that 1-ethynylpyrene shows a one-electron oxidation step at 1.42 V *vs.* Ag/AgCl, which is clearly assignable to the pyrene unit.[21] A similar oxidation step is seen for the analogous pyrene-thiophene dyad $\mathbf{L_2}$, where the first oxidation peak occurs at 1.25 V *vs.* Ag/AgCl. Again, this peak is assigned to one-electron oxidation of the pyrene unit. There is a second oxidation peak for $\mathbf{L_2}$, which occurs at 1.63 V *vs.* Ag/AgCl and is attributed to one-electron oxidation of the thiophene group. Oxidation of the thiophene unit in $\mathbf{L_1}$ can be observed at *ca.* 2.0 V *vs.* Ag/AgCl, although this is very close to the onset of solvent oxidation. Presumably, the second ethynylene group is responsible for raising the oxidation potential of the thiophene group. Addition of $Zn(ClO_4)_2$ to the solution of $\mathbf{L_1}$ has no obvious effect on the oxidative processes.

One-electron reduction of 1-ethynylpyrene[21] occurs with a half-wave potential ($E_{1/2}$) of -1.73 V *vs.* Ag/AgCl while the corresponding compound having a terminal 2,2′-bipyridine group exhibits two reduction steps. The first reduction has $E_{1/2} = -1.63$ V *vs.* Ag/AgCl and has been assigned to reduction of the bipyridyl unit. The second reduction step takes place with $E_{1/2} = -1.88$ V *vs.* Ag/AgCl and was attributed to reduction of the pyrene residue.[21] In this latter compound, reduction of the pyrene group is made more difficult because of extensive electron delocalisation along the molecular axis following addition of the first electron.

In comparison, $\mathbf{L_1}$ exhibits a poorly reversible ($\Delta E_p = 140$ mV) wave with $E_{1/2} = -1.61$ V *vs.* Ag/AgCl. At more cathodic potentials, a second reduction process occurs with $E_{1/2} = -1.90$ V *vs.* Ag/AgCl. The marked similarity with the bipyridine-based compound mentioned above suggests that the first electron should go to the terminal terpyridyl unit. However, molecular orbital calculations made after energy-minimisation of the ground-state conformation of $\mathbf{L_1}$ in a bath of water molecules show that the LUMO is clearly associated with the central thiophene unit. The terminal terpyridyl group does not contribute significantly towards the LUMO. Interestingly, LUMO(1) contains a major contribution from the terpyridyl residue, with some participation from the pyrene terminal. On this basis, the central thiophene residue will be reduced before or immediately after the terpyridyl terminal. This effect results from attaching two ethynylene groups to the thiophene residue. Clearly, electron delocalisation will affect the reduction potential of the terpyridine group, making it more difficult to reduce than expected from the reference compound.[21]

The corresponding pyrene-thiophene dyad $\mathbf{L_2}$ shows a quasi-reversible reductive process with $E_{1/2} = -1.59$ V *vs.* Ag/AgCl. This step is assigned to one-electron reduction of the pyrene moiety, rather than reduction of the thiophene residue. Support for this hypothesis comes from the observation that the absorption and fluorescence spectra show no obvious indications for an intramolecular charge-transfer band, in contrast to $\mathbf{L_1}$. Furthermore, molecular orbital calculations made *in vacuo* for the energy-minimised geometry indicate that both the HOMO and the LUMO are localised mostly on the pyrene unit of $\mathbf{L_2}$, with little contribution from the thiophene moiety. The same calculations made in a polar solvent indicate increased contribution from the thiophene residue but still point towards the first-excited state being primarily of π,π^* character. The first spin-allowed absorption transition calculated from these MO studies, and allowing for configuration interaction with five occupied and six empty orbitals in active space, is at 400 nm. This value is in good agreement with the experimental result of 392 nm. As such, the calculations appear to be reliable.

Addition of a slight excess of $Zn(ClO_4)_2$ to a solution of $\mathbf{L_1}$ perturbs the cyclic voltammograms observed upon reductive scans. The most notable effect is the appearance of a broad, quasi-reversible peak centred at -1.28 V *vs.* Ag/AgCl. This peak corresponds to two overlapping reduction steps, each of which is due to the transfer of one electron. There is extensive

literature evidence to indicate that coordination of a cation has a marked effect on the reduction potential of poly(pyridines).[29,38] As such, we can surmise that complexation of $Zn(ClO_4)_2$ pushes the half-wave potential for reduction of the terpyridine unit to a much less negative value. The two overlapping peaks, therefore, can be assigned to one-electron reduction of the coordinated terpyridyl terminal and the central thiophene unit.

Several pieces of evidence lead us to conclude that the first reduction process found for L_1 in the presence of a slight excess of $Zn(ClO_4)_2$ corresponds to reduction of the resultant metal complex. Firstly, this step is quasi-reversible whereas reduction of the thiophene unit in L_1 is poorly reversible. Secondly, molecular-orbital calculations indicate that the LUMO becomes localised on the metal complex following attachment of the cation. Finally, the absorption and fluorescence spectral measurements (see later) show that cation complexation causes severe perturbation of the internal electronic sysem. This latter effect is most easily explained in terms of a charge-shift reaction that requires the metal complex to be the most easily reduced subunit.

The second reduction step for L_1, which overlaps with that assigned to reduction of the metal complex, can now be assigned to one-electron reduction of the central thiophene unit. The half-wave potential for this latter step is less negative by *ca.* 200 mV than that found in the absence of Zn^{2+} cations. This effect can be explained in terms of a cation-induced charge-shift reaction. Thus, the ground state of L_1 in a polar solvent can be considered to involve a substantial amount of charge-transfer character whereby electronic charge is transferred from the pyrene terminal to the central thiophene residue. Such charge transfer will partially offset the electronic effect of the ethynylene groups and render reduction somewhat more difficult. Upon coordination of the cation, the terminal metal complex becomes easier to reduce than the central thiophene unit and, accordingly, charge is transferred to the metal complex. It is likely that this electron is localised by strong electrostatic attraction provided by the dication. As such, the thiophene residue will become less difficult to reduce. Support for this hypothesis arises from the ^1H NMR studies that clearly indicate an upfield shift for the thiophene proton upon cation binding.

The cyclic voltammograms indicate that coordination of Zn^{2+} cations lowers the reduction potential for the terpyridyl group by >600 mV. Indeed, complexation can be followed by monitoring the peak current at −1.3 V *vs.* Ag/AgCl as a function of the concentration of added $Zn(ClO_4)_2$. The electrochemical process is quasi-reversible and does not result in irreversible reduction of the compound. As such, L_1 can be considered to function as an electrochemical sensor for added zinc(II) cations.

Electrospray mass spectrometry

To ascertain the stoichiometry of the complex(es) formed with zinc(II) cations, electrospray mass spectrometry (ES-MS) was perfomed for CH_3CN solutions containing L_1 and $Zn(ClO_4)_2$ in molar ratios of 1 : 1 and 2 : 1, respectively. For the equimolar solution, a cluster of peaks is evident at $m/z = 368.7$ which can be assigned to the dicationic species $[ZnL_1(CH_3CN)_2]^{2+}$. A further cluster of peaks is observed at $m/z = 756.2$, which fits well with the theoretical pattern predicted for the monocationic species $[ZnL_1]ClO_4^+$. In comparison, the 2 : 1 (ligand : metal) solution displayed peaks centred at 624.1, which correspond to the theoretical pattern calculated for the monocationic complex $[Zn(L_1)_2]ClO_4^+$.

Evidently, at high ligand : metal stoichiometry, the dominant species in solution is $[Zn(L_1)_2]^{2+}$. This latter species reacts with added metal cation to form the analogous $[ZnL_1]^{2+}$ complex. It is interesting to note that the ES-MS profiles show little

indication for the co-existence of 1 : 1 and 1 : 2 (metal : ligand) complexes under these conditions.

Photophysical properties

The absorption spectrum recorded for L_1 in acetonitrile solution shows a series of transitions between 200 and 450 nm. The lowest-energy transition is of intramolecular charge-transfer character and is centred at 426 nm (Fig. 2). This absorption maximum is in excellent agreement with that calculated from the MO studies where the transition is predicted to occur at 432 nm. The molar absorption coefficient for the first-allowed transition is 19 550 $mmol^{-1}$ cm^2. According to our interpretation of the cyclic voltammograms, the electron donor is the pyrene terminal whilst the electron acceptor will be the central thiophene residue (Scheme 3). Of course, there is extensive electron delocalisation over these subunits such that the exact nature of the donor and acceptor cannot be properly defined. As might be expected on the basis of the MO calculations, the absorption spectrum recorded for L_2 is quite different (Fig. 3). Here, the lowest-energy absorption band is assigned to a π,π^* transition.
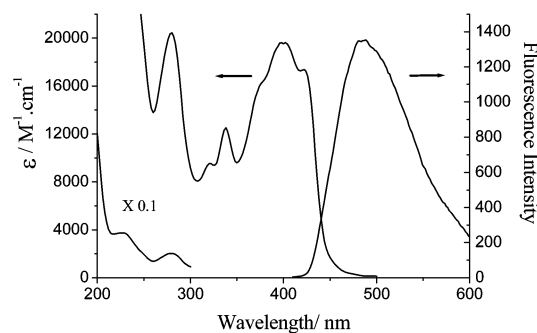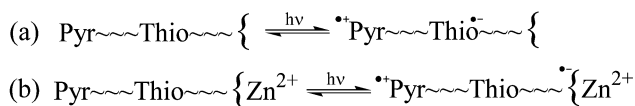
Fig. 2 Absorption and fluorescence spectra recorded for L_1 in dilute acetonitrile solution.

Scheme 3 Pictorial representation of the proposed intramolecular charge transfer in (a) L_1 and (b) the Zn^{2+} complex formed from L_1.

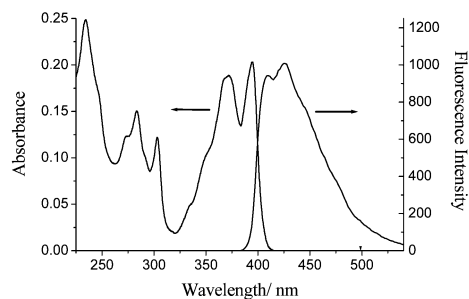**Fig. 3** Absorption and fluorescence spectra recorded for L_2 in dilute acetonitrile solution.

Addition of $Zn(ClO_4)_2$ to a solution of L_1 had a large effect over much of the spectral range. The lowest-energy transitions are shifted towards longer wavelength and lose some of their fine structure (Fig. 4). This red shift is accompanied by a substantial increase in absorptivity over the 400–500 nm range. These spectral changes are consistent with complexation making the electron acceptor more electron affinic. On the basis of the MO calculations and the cyclic voltammograms, it appears that coordination of Zn^{2+} makes the terpyridine unit the most easily reduced subunit. As such, we can suppose that charge is transferred from pyrene to the metal complex once the
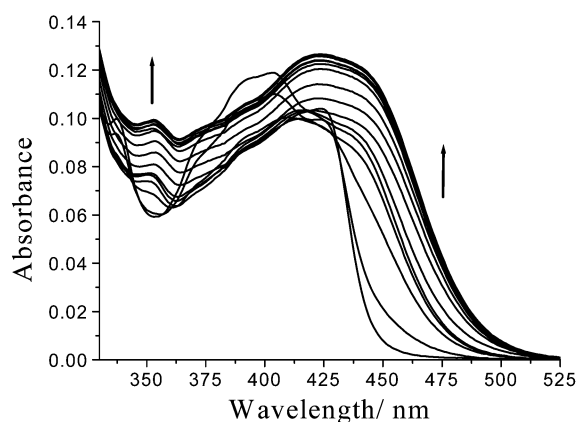
Fig. 4 Spectrophotometric titration showing successive addition of $Zn(ClO_4)_2$, over the range 0–100 µM, to a solution of L_1 in acetonitrile. Complexation is accompanied by a large increase in absorbance around 450 nm.
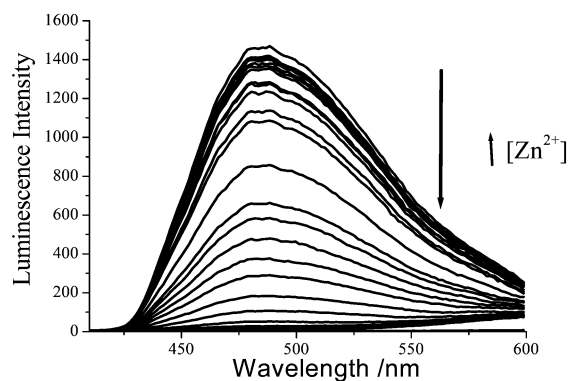

Fig. 5 Fluorescence titration of L_1 with $Zn(ClO_4)_2$ in acetonitrile solution. Addition of cation, over the range 0–20 µM, causes extinction of the fluorescence band centred around 480 nm but appearance of a band centred at 600 nm. Further addition of $Zn(Cl_4)_2$ causes the latter band to disappear.

cation has been attached. Monitoring at 460 nm allows clean detection of the cationic complex. Addition of $Zn(ClO_4)_2$ to L_2 in acetonitrile solution has no obvious effect on the absorption spectrum.

The new absorption band observed at long wavelength in the presence of $Zn(ClO_4)_2$ does not resemble the well-known[25] absorption spectrum of $[Zn(terpy)_2]^{2+}$. The molar absorption coefficient at the apparent maximum of 440 nm is 36 035 mmol^{-1} cm². According to the stability constants derived later, this species is the 1 : 1 complex. The lowest-energy absorption band can be approximated to a broad Gaussian-shaped profile with a maximum at 437 nm and a half-width of 2930 cm^{-1}. As such, it seems reasonable to suppose that this absorption band corresponds to an intramolecular charge-transfer transition.[39] The most reasonable interpretation of the experimental data has pyrene as the electron donor and the metal complex as the ultimate electron acceptor (Scheme 3). Thus, the effect of cation coordination is to shift the charge from the central thiophene unit to the terminal metal complex. The result is a giant dipole along the molecular axis.

In acetonitrile solution at ambient temperature, L_1 displays intense fluorescence centred around 488 nm (Fig. 2). The fluorescence quantum yield is 0.32 while the fluorescence lifetime is 1.2 ns. The fluorescence intensity was unaffected by the presence of molecular oxygen, presumably because of the relatively short excited state lifetime. Comparison of absorption and emission spectral profiles indicates that there is a substantial Stokes' shift (*i.e.*, *ca.* 62 nm) in acetonitrile. This finding is consistent with fluorescence arising from a charge-transfer state. The fluorescence excitation spectrum matches the absorption profile over the range 250 to 450 nm. The fluorescence spectrum is broad and fairly structureless. It does not resemble a mirror image of the lowest-energy absorption band. Taken together with the large Stokes's shift, this finding suggests to us that there is a significant geometry change after excitation.

In contrast, the fluorescence spectrum recorded for the control ligand L_2 shows a relatively small Stokes shift (Fig. 3) that increases with increasing polarity of the solvent. There are indications for mixing between a π,π^* excited state and an intramolecular charge-transfer state in polar solvents. In particular, the fluorescence and absorption profiles do not show good mirror symmetry. Such behaviour has been observed in many molecular dyads.[40] It is likely that charge transfer requires the molecule to adopt a preferred geometry.

Addition of $Zn(ClO_4)_2$ to the solution of L_1 causes a severe decrease in the fluorescence yield (Fig. 5). The fluorescence band centred at 488 nm diminishes progressively with increasing concentration of cation. However, at low concentration of $Zn(ClO_4)_2$ the spectral profiles show the appearance of a weak
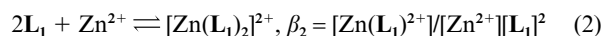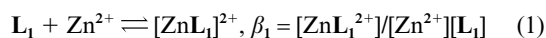
emission band centred around 600 nm. This latter emission is difficult to resolve from the baseline but is attributed to fluorescence from the resultant $[Zn(terpy)_2]^{2+}$ complex. As the concentration of added $Zn(ClO_4)_2$ increases there is a progressive extinction of this new fluorescence band. Taken together with the ES-MS results, this finding indicates that the 1 : 1 complex does not emit. Addition of $Zn(ClO_4)_2$ to a solution of L_2 in acetonitrile has little, if any, effect on the fluorescence yield.

The fluorescence spectral profile recorded after addition of sufficient $Zn(ClO_4)_2$ to form the 1 : 2 (metal : ligand) complex is independent of excitation wavelength. Furthermore, the corrected excitation spectrum agrees well with the absorption spectrum recorded over the 300–500 nm range. Under these conditions, the fluorescence quantum yield is *ca.* 0.006 but no low-temperature phosphorescence could be detected at $\lambda < 750$ nm. It seems likely that deactivation of the excited state involves rapid charge recombination to restore the ground state. In this case, the shorter fluorescence lifetime relative to L_1 could be explained in terms of the energy-gap law.[41] It appears that the 1 : 1 complex does not emit under these conditions.

Complexation studies

As noted above, addition of $Zn(ClO_4)_2$ to a solution of L_1 in acetonitrile causes largescale changes in the absorption spectrum. These changes were analysed as a function of the amount of added salt in order to obtain estimates for stability constants of the 1 : 1 and 1 : 2 (metal : ligand) complexes identified in the ES-MS studies. In order to properly fit the titration data, a vector analysis indicates that three absorbing species are necessary; namely, the free ligand L_1, for which the absorption spectrum is known, and two metal complexes. These latter complexes possess similar absorption spectra. The best fit to the experimental data gives $\log\beta_1 = 5.10 \pm 0.12$ and $\log\beta_2 = 9.90 \pm 0.15$ (eqns. (1) and (2))

$$L_1 + Zn^{2+} \rightleftharpoons [ZnL_1]^{2+}, \beta_1 = [ZnL_1^{2+}]/[Zn^{2+}][L_1] \quad (1)$$

$$2L_1 + Zn^{2+} \rightleftharpoons [Zn(L_1)_2]^{2+}, \beta_2 = [Zn(L_1)^{2+}]/[Zn^{2+}][L_1]^2 \quad (2)$$

.

A fluorescence titration was made for addition of low concentrations of $Zn(ClO_4)_2$ to a solution of L_1 in acetonitrile at room temperature (Fig. 5). The emission yield falls steeply with increasing concentration of cation, reaching a plateau value. Taking due account of the above results, it seems appropriate to consider formation of both 1 : 1 and 1 : 2 (metal : ligand) complexes. Thus, iterative fitting of the experimental data to such a model allows calculation of the overall stability constants $\log\beta_1$ and $\log\beta_2$ as being 6.1 ± 0.5 and 11.0 ± 0.7, respectively (Fig. 6). This analysis is made on the basis that the 1 : 2 complex fluoresces weakly but that the 1 : 1 complex does not
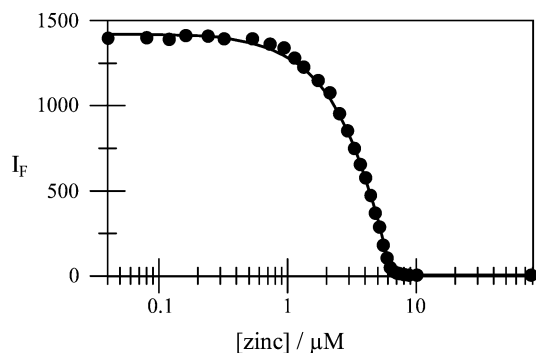
Fig. 6 Fluorescence titration recorded following successive addition of zinc perchlorate to a solution of L_1 in acetonitrile. The solid line drawn through the data points is a linear-least squares fit to the binding constants given in the text. The fluorescence intensity (I_F) was measured ar 470 nm following excitation at 370 nm.

emit over the 400–700 nm spectral range. The results obtained with L_2 suggests that Zn^{2+} binds only very weakly, if at all, to the thiophene residue.

The derived stability constants appear to be in line with values reported for related terpyridine ligands.[42] Addition of the second ligand is very slightly less favourable than for the first ligand and there is no obvious indication of cooperativity. The stability constants derived from the fluorescence titration are in reasonable agreement with those obtained by UV-visible spectrophotometry. The fluorescence results are less accurate, however, because fewer wavelengths were analysed and the spectral changes were less pronounced than those seen in the UV-visible titrations, where clear intermediate species can be resolved. Furthermore, the fluorescence titrations require lower concentrations of fluorophore and cation, making the impact of trace impurities more important. Better agreement with the results of the UV-visible titrations was obtained if the fluorescence data were analysed at 475 nm where only the free ligand emits to a significant degree. An additional complication for the fluorescence studies concerns the fact that the absorption spectrum changes during the titration. There is no clear isosbestic point that can be used as excitation wavelength. This does not affect the reproducibility of the fluorescence titrations, which is excellent, but affects the values of the derived stability constants. The stability constants derived by UV-visible titration are considered to be the more reliable values.

Attempts to measure the rate of complexation between L_1 and Zn^{2+} cations in acetonitrile at ambient temperature were unsuccessful. Even at low concentrations of Zn^{2+}, and with $[L_1] < [Zn^{2+}]$, the reaction was complete within 2 ms. From the stopped-flow studies, made using absorbance changes around 500 nm, it was concluded that the bimolecular rate constant for complexation exceeds 6×10^7 dm^3 mol^{-1} s^{-1} at 20 °C.

Concentration profiles

The fact that L_1 forms both 1 : 1 and 1 : 2 (metal : ligand) complexes with added Zn^{2+} cations helps to extend the concentration range over which the reporter can operate. At low cation concentrations, the dominant species will be the 1 : 2 complex but the high stability constant found for this species means that only low concentrations of Zn^{2+} cations are needed to reduce the concentration of free ligand (Fig. 7). As the concentration of Zn^{2+} cations increases, the 1 : 2 complex is disfavoured with respect to the 1 : 1 complex. Because of the relative stability constants, the equimolar position is reached at quite low cation concentration. Thus, the 1 : 1 complex emerges early in the titration. The key observation regarding the putative design of an efficient fluorescence sensor is that the concentration of L_1 decreases sharply with increasing cation concentration. Indeed, the free ligand is diminished to <5% of its initial concentration when the metal : ligand molar ratio exceeds 4 (Fig. 7).
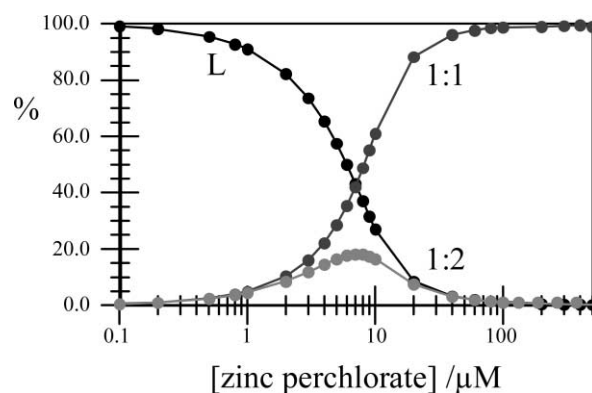
Fig. 7 Concentration profiles calculated for the free ligand (L_1), the 1 : 1 complex and the 1 : 2 complex on the basis that $\log\beta_1$ and $\log\beta_2$, respectively, have values of 5.5 and 10.5. Values were obtained by numerical solution of the model equations.

Conclusions

We have demonstrated that L_1 binds adventitious Zn^{2+} cations in the form of 1 : 1 and 1 : 2 (metal : ligand) complexes. The free ligand is highly fluorescent due to the efficient population of an intramolecular charge-transfer excited state. Coordination of Zn^{2+} cations to the vacant terpyridyl terminal serves to raise the reduction potential of the poly(pyridine) unit and thereby direct the promoted electron from the central thiophene unit to the terminal metal complex. The net result is a serious extinction of the fluorescence yield. Complexation can also be followed by UV-visible absorption spectroscopy and by electrochemical reduction. As such, L_1 represents a versatile chemical sensor for Zn^{2+} cations in solution. The overall stability constants are high, ensuring good sensitivity, and there is a large variation in fluorescence yield upon complexation of the cation. This latter condition represents the "off–on" situation and is critical for the design of an efficacious fluorescence sensor. In the case of L_1, the "off" signal is set by fluorescence from the zinc complex, which corresponds to ca. 3% of the the free ligand. It is possible to improve this "on–off" ratio by monitoring at 470 nm where the resultant zinc complex does not emit.

The sensor is not expected to display selectivity towards particular cations in solution, although there will be a large variation in the stability constants for coordination of different species. Preliminary studies have indicated that L_1 responds to numerous cations (e.g., Na^+, H^+, Ca^{2+}, Li^+, Ba^{2+} and Al^{3+}) in much the same way as described herein for Zn^{2+}. The sensor is especially responsive towards Fe^{2+}. It has also been observed that L_1 is able to transport K^+ cations across a liquid membrane with reasonable efficacy. Finally, we note that the favourable electrode potentials and intense luminescence found for L_1 suggests its possible use in electrogenerated luminescence devices. These, and related studies, are on-going.

References

1 (a) A. S. Klymchenko and A. P. Demchenko, *J. Am. Chem. Soc.*, 2002, **124**, 12372; (b) G. Hennrich, H. Sonnenschein and U. Resch-Genger, *J. Am. Chem. Soc.*, 1999, **121**, 5073.
2 H. F. M. Nelissen, M. Kercher, L. De Cola, M. C. Feiters and R. J. M. Nolte, *Chem. Eur. J.*, 2002, **8**, 5407.
3 (a) S. L. Murphy, S. J. Loeb and G. K. H. Shimizu, *Tetrahedron*, 1998, **54**, 15137; (b) P. D. Beer and K. Y. Wild, *Polyhedron*, 1996, **15**, 775; (c) P. D. Beer, M. G. B. Drew, R. J. Knubley and M. I. Ogden,

J. Chem. Soc., Dalton Trans., 1995, 3117; (*d*) P. D. Beer, E. L. Tite and A. Ibbotson, *J. Chem. Soc., Dalton Trans.*, 1991, 1691.

4 (*a*) A. L. Gott, P. C. McGowan, T. J. Podesta and M. Thornton-Pett, *J. Chem. Soc., Dalton Trans.*, 2002, 3619; (*b*) A. J. Blake, J. P. Danks, W. S. Li, V. Lippolis and M. Schröder, *J. Chem. Soc., Dalton Trans.*, 2000, 3034; (*c*) C. Bazzicalupi, A. Bencini, A. Bianchi, V. Fedi, V. Fusi, C. Giorgi, P. Paoletti, L. Tei and B. Valtancoli, *J. Chem. Soc., Dalton Trans.*, 1999, 1101; (*d*) S. Ogawa and S. Tsuchiya, *Chem. Lett.*, 1996, 709; (*e*) A. J. Blake, I. A. Fallis, S. Parsons, S. A. Ross and M. Schröder, *J. Chem. Soc., Dalton Trans.*, 1996, 525; (*f*) A. Liebmann, C. Mertesdorf, T. Plesnivy, H. Ringsdorf and J. H. Wendorff, *Angew. Chem., Int. Ed. Engl.*, 1991, **30**, 1375.

5 T. Schneppensieper, S. Finkler, A. Czap, R. van Eldik, M. Heus, P. Nieuwenhuizen, C. Wreesmann and W. Abma, *Eur. J. Inorg. Chem.*, 2001, 491.

6 (*a*) G. T. Hwang and B. H. Kim, *Tetrahedron*, 2002, **58**, 9019; (*b*) P. A. Gale, Z. Chen, M. G. B. Drew, J. A. Heath and P. D. Beer, *Polyhedron*, 1998, **17**, 405; (*c*) J. B. Lambert, C. Q. Liu, M. T. Boyne, A. P. Zhang and Y. X. Yin, *Chem. Mater.*, 2003, **15**, 131; (*d*) H. Halouani, I. Dumazet-Bonnamour, C. Duchamp, C. Bavoux, N. Ehlinger, M. Perrin and R. Lamartine, *Eur. J. Org. Chem.*, 2002, 4202; (*e*) A. Specht, P. Bernard, M. Goeldner and L. Peng, *Angew. Chem., Int. Ed.*, 2002, **41**, 4706.

7 (*a*) Y. Yuan, G. Gao, Z. L. Jiang, J. S. You, Z. Y. Zhou, D. Q. Yuan and R. G. Xie, *Tetrahedron*, 2002, **58**, 8993; (*b*) R. Breslow and Z. L. Fang, *Tetrahedron Lett.*, 2002, **43**, 5197; (*c*) S. S. Sun, J. A. Anspach, A. J. Lees and P. Y. Zavalij, *Organometallics*, 2002, **21**, 685; (*d*) A. Dalla Cort, M. Nissinen, D. Mancinetti, E. Nicoletti, L. Mandolini and K. Rissanen, *J. Phys. Org. Chem.*, 2001, **14**, 425; (*e*) M. Nissinen, A. Dalla Cort, S. Amabile, L. Mandolini and K. Rissanen, *J. Inclusion Phenom. Macrocycl. Chem.*, 2001, **39**, 229; (*f*) Y. Tobe, N. Utsumi, A. Nagano and K. Naemura, *Angew. Chem., Int. Ed.*, 1998, **37**, 1285; (*g*) A. C. Benniston, P. R. Mackie and A. Harriman, *Tetrahedron Lett.*, 1997, **38**, 3577.

8 R. J. M. K. Gebbink, S. I. Klink, M. C. Feiters and R. J. M. Nolte, *Eur. J. Inorg. Chem.*, 2000, 253.

9 N. J. van der Veen, E. Rozniecka, L. A. Woldering, M. Chudy, J. Huskens, F. C. J. M. van Veggel and D. N. Reinhoudt, *Chem. Eur. J.*, 2001, **7**, 4878.

10 R. H. Yang, W. H. Chan, A. W. M. Lee, P. F. Xia, H. K. Zhang and K. A. Li, *J. Am. Chem. Soc.*, 2003, **125**, 2884.

11 (*a*) G. Bobba, R. S. Dickins, S. D. Kean, C. E. Mathieu, D. Parker, R. D. Peacock, G. Siligardi, M. J. Smith, J. A. G. Williams and C. F. G. C. Geraldes, *J. Chem. Soc., Perkin Trans. 2*, 2001, 1729; (*b*) R. S. Dickens, J. A. K. Howard, C. L. Maupin, J. M. Moloney, D. Parker, R. D. Peacock, J. P. Riehl and G. Siligardi, *New J. Chem.*, 1998, **22**, 891.

12 (*a*) R. S. Dickins, S. Aime, A. S. Batsanov, A. Beeby, M. Botta, J. Bruce, J. A. K. Howard, C. S. Love, D. Parker, R. D. Peacock and H. Puschmann, *J. Am. Chem. Soc.*, 2002, **124**, 12697; (*b*) J. I. Bruce, R. S. Dickins, L. J. Govenlock, T. Gunnlaugsson, S. Lopinski, M. P. Lowe, D. Parker, R. D. Peacock, J. J. B. Perry, S. Aime and M. Botta, *J. Am. Chem. Soc.*, 2000, **122**, 9674.

13 For reviews, see: (*a*) A. P. de Silva, H. Q. Nimal Gunaratne, T. Gunnlaugsson, A. J. M. Huxley, C. P. McCoy, J. T. Rademacher and T. E. Rice, *Chem. Rev.*, 1997, **97**, 1515; (*b*) B. Valeur and I. Leray, *Coord. Chem. Rev.*, 2000, **205**, 3; (*c*) L. Prodi, F. Bolletta, M. Montalti and N. Zaccheroni, *Coord. Chem. Rev.*, 2000, **205**, 59.

14 G. P. Zanini, H. A. Montejano and C. M. Previtali, *J. Photochem. Photobiol. A: Chem.*, 2000, **132**, 161.

15 A-J. Tong, A. Yamauchi, T. Hayashita, Z-Y. Zhang, B. D. Smith and N. Termae, *Anal. Chem.*, 2001, **73**, 1530.

16 (*a*) J. S. Kim, O. J. Shon, J. A. Rim, S. K. Kim and J. Yoon, *J. Org. Chem.*, 2002, **67**, 2348; (*b*) T. Jin, *Chem. Commun.*, 1999, 2491.

17 A. Corma, M. S. Galletero, H. García, E. Palomares and F. Rey, *Chem. Commun.*, 2002, 1100.

18 Y. Fujiwara, I. Okura, T. Miyashita and Y. Amao, *Anal. Chim. Acta.*, 2002, **471**, 25.

19 L. J. D'Souza and U. Maitra, *J. Org. Chem.*, 1996, **61**, 9494.

20 D. Y. Sakaki and B. E. Padilla, *Chem. Commun.*, 1998, 1581.

21 A. Harriman, M. Hissler and R. Ziessel, *Phys. Chem. Chem. Phys.*, 1999, **1**, 4203.

22 P. Richter, M. I. Toral, A. E. Tapia and E. Fuenzalida, *Analyst*, 1997, **122**, 1045.

23 E. Kimura and T. Koike, *Chem. Commun.*, 1998, 1495.

24 S. Charles, F. Dubois, S. Yunus and E. Vander Donckt, *J. Fluoresc.*, 2000, **10**, 99.

25 G. Albano, V. Balzani, E. C. Constable, M. Maestri and D. R. Smith, *Inorg. Chim. Acta*, 1998, **277**, 225.

26 S. Leroy, T. Soujanya and F. Fages, *Tetrahedron Lett.*, 2001, **42**, 1665.

27 D. D. Perrin and W. L. F. Armarego, *Purification of Laboratory Chemicals*, Permagon Press Ltd., Oxford, 3rd edn., 1988.

28 D. L. Pearson and J. M. Tour, *J. Org. Chem.*, 1997, **62**, 1376.

29 M. Hissler, A. Harriman, A. Khatyr and R. Ziessel, *Chem. Eur. J.*, 1999, **5**, 3366.

30 K. T. Potts and D. Konwar, *J. Org. Chem.*, 1991, **56**, 4815.

31 T. Suzuki, M. Nagano, S. Watanabe and T. Ichimura, *J. Photochem. Photobiol. A, Chem.*, 2000, **136**, 7.

32 J. V. Caspar and T. J. Meyer, *J. Am. Chem. Soc.*, 1983, **105**, 5583.

33 Y. Harima, X. Jiang, Y. Kuniga, K. Yamashita, A. Naka, K. K. Lee and M. Ishikawa, *J. Mater. Chem.*, 2003, **13**, 1298.

34 S. Y. Yang, G. A. Sotzing and M. Marquez, *Macromolecules*, 2002, **35**, 7293.

35 K. Sonogashira, Y. Tohda and N. Hagihara, *Tetrahedron Lett.*, 1975, **16**, 4467.

36 M. A. McCoy and D. F. Wyss, *J. Am. Chem. Soc.*, 2002, **124**, 11758.

37 J. L. Sessler, Y. Kubo and A. Harriman, *J. Phys. Org. Chem.*, 1992, **5**, 644.

38 L. M. Voger, S. W. Jones, G. E. Jensen, G. Brewer and K. J. Brewer, *Inorg. Chim. Acta.*, 1996, **250**, 155.

39 L. Tan, M. D. Curtis and A. H. Francis, *Macromolecules*, 2002, **35**, 4628.

40 (*a*) D. Lui, J. Li, H. Pan, Y. Li, Z-X. Guo and D. Zhu, *Synth. Met.*, 2003, **135–136**, 851; (*b*) H. Tian, W. Ni, J. Su and K. Chen, *J. Photochem. Photobiol. A: Chem.*, 1997, **109**, 213.

41 (*a*) T. Asahi and N. Mataga, *J. Phys. Chem.*, 1989, **93**, 6575; (*b*) H. Segawa, C. Takehara, K. Honda, T. Shimidzu, T. Asahi and N. Mataga, *J. Phys. Chem.*, 1992, **96**, 503; (*c*) R. Englman and J. Jortner, *J. Mol. Phys.*, 1970, **18**, 145.

42 W. Goodhall and J. A. G. Williams, *Chem. Commun.*, 2001, 2514.